# Shaping of nanostructured materials or coatings through Spark Plasma Sintering

C. Estournès[1], D. Oquab[2], S. Selezneff[2], M. Boidot[2], D. Monceau[2], D. Grossin[2], C. Drouet[2], U-Chan Chung[3], F. Roulland[1,3], C. Elissalde[3], M. Maglione[3], R. Chaim[4], Ph. Miele[5], J. Gurt-Santanach[6], G. Chevallier[1], A. Weibel[6], A. Peigney[6] and Ch. Laurent[6]

[1] CNRS, Institut Carnot CIRIMAT, 31062 Toulouse cedex 9, France
[2] Université de Toulouse, UMR CNRS-UPS-INP 5085, CIRIMAT, INPT-ENSIACET, 4, allé Emile Monso, BP 74233, 31432 Toulouse cedex 4, France
[3] ICMCB-CNRS, Université Bordeaux, 87 Avenue du Dr A. Schweitzer, F-33608 Pessac Cedex, France
[4] Department of Materials Engineering, Technion – Israel Institute of Technology, Haifa 32000, Israel
[5] LMI, UMR CNRS 5615, Université Claude Bernard-Lyon 1, 43 bvd du 11 novembre 1918, 69622 Villeurbanne Cedex, France
[6] Université de Toulouse, UMR CNRS-UPS-INP 5085, CIRIMAT, Université Paul-Sabatier, Bât. 2R1, 118 route de Narbonne, 31062 Toulouse cedex 9, France

**Kewords**: Nanomaterials, Spark Plasma Sintering, Mechanisms, Ceramics, Coatings

**Abstract** In the field of advanced ceramics, Spark Plasma Sintering (SPS) is known to be very efficient for superfast and full densification of ceramic nanopowders. This property is attributed to the simultaneous application of high density dc pulsed current and load, even though the sintering mechanisms involved remain unclear. In the first part of the paper, the mechanisms involved during SPS of two insulating oxide nanopowders ($Al_2O_3$ and $Y_2O_3$) are discussed while in the second part illustrations of the potential of SPS will be given for (i) Consolidation of mesoporous or unstable nanomaterials like SBA-15 or biomimetic apatite, respectively; (ii) Densification of core (BT or BST)/shell ($SiO_2$ or $Al_2O_3$) nanoparticles with limited or controlled reaction at the interface. (iii) *In-situ* preparation of surface-tailored Fe–$FeAl_2O_4$–$Al_2O_3$ nanocomposites, and finally (iv) One-step preparation of multilayer materials like a complete thermal barrier system on single crystal Ni-based superalloy.

## Introduction

Nanostructured materials have benefited from considerable development these last decades. Their fields of application are extremely vast since they extend from optoelectronics to biomaterials. In the isolated state, their specificity is particularly due to the fact that their small size can generate confinement phenomena but also because their surfaces/interfaces may exert multiple influences on their properties. The nature of these clusters, particles or grains is variable: for instance polymers, metals, “ceramics”, dielectrics, magnetic oxides, ordered silicates, carbon nanotubes. Their individual nature affects the mechanical, optical, magnetic, thermodynamic, catalytic and chemical properties. One of the objectives of material scientists is to transpose the specific properties of these divided states of matter to the macroscopic scale. Even though nonconventional techniques have significantly reduced the characteristic sintering times, a crucial problem remains to be solved. For the shaping of these objects, the various treatments should not involve their deterioration and/or the loss of the divided state which would imply the disappearance of their specific properties. Over recent years, much progress has been made in the methods used for the consolidation of nanocristalline powders. Thus, fast techniques of consolidation [1], sintering at high pressures [2], liquid phase assisted sintering [3] and low-temperature two-step sintering [4]have allowed the preparation of dense ceramics, but the success depends largely on the

technique used. In addition to the temperature, one of the factors limiting the traditional sintering of nano-powders, even under pressure, is obviously the duration of the cycle. It is consequently necessary to turn to techniques requiring shorter processing times. One of these techniques of rapid consolidation is “Spark Plasma Sintering” (SPS) because it accelerates the sintering kinetics and thus reduces the time available for grain growth.

**SPS technology**

One of the methods used to accelerate the kinetics of sintering is to apply an electrical current. This idea is not new since the first reports in the literature go back to 1906 with two patents of Bloxam [5,6] reporting the manufacture of bulb tungsten filaments by direct passage of an electrical current. Various work were then undertaken to improve this technique [7]. At the end of the sixties, Inoue patented the technique known as *Spark Plasma Sintering* [8,9] The basic idea was to develop a machine able to create a plasma via an electric discharge during sintering under pressure of metals and ceramics. Inoue's idea was that plasma-assisted sintering could enable the preparation of new materials. Many alternative forms of SPS were attempted over the last decades under different names *Plasma-Assisted Sintering* (PAS) [10], *Pulsed Electric Current Sintering* (PECS) [11], *Electroconsolidatio*n or *Electric Pulse Assisted Consolidation* (EPAC) [12], and the original *Spark Plasma Sintering* (SPS) [13].

The SPS process is in appearance very similar to hot pressing (HP) [7] because the precursors (generally without any sintering additives) are introduced into a die on which a uniaxial pressure (up to few hundred MPa depending on the process) can be applied during the thermal cycle. These dies are introduced into a chamber where sintering is usually carried out under vacuum (down to $6.10^{-3}$ Pa), but it can also be under neutral (argon, nitrogen), reducing (hydrogen) or even under oxidizing atmospheres (air) but in the last case, over a few hundred of degrees Celsius, the die can no longer be made of graphite.

The major difference between HP and SPS lies in the fact that the heating source is not external but an electrical current (direct - direct pulsed - or alternative) is passed through the conducting dies and sometimes through the sample when it is also conducting. In most current SPS devices, lines of dc pulsed current, interspersed with dead times, of variables intensity and voltages are applied to reach the desired sintering temperature. The waveform of the pulsed sequence varies depending on the manufacturer of the machine. Whatever the configuration of the machine, very high rates of increasing/decreasing temperature (up to 1000°C/min and more) are achieved while ensuring good heat transfer to the sample.

**Sintering Mechanisms**

In spite of numerous publications during the last decade highlighting the undeniable sintering performances of SPS, very few attempt to understand the underlying sintering mechanisms.

Olevski proposed a first model of SPS sintering based on those existing for traditional sintering but considered only the high heating rate available on SPS and did not take into account certain aspects, especially the potential gradient applied to the materials[14,15]. In any case, it appears that his model is in agreement with the results of SPS densification of aluminium powder.

Bernard-Granger *et al.* tried to analyze SPS and HP sintering behavior of a commercial yttrium-stabilized zirconia powder using the creep models developed in the past for hot pressing [16]. For this material, even though the sintering trajectories obtained by SPS and HP are identical, these authors report that the densification mechanisms involved are not exactly the same. They mention that HP densification proceeds by grain boundary sliding accommodated either by grain boundary diffusion of $Zr^{4+}$ and/or $Y^{3+}$ cations or by an in-series (interface-reaction/lattice diffusion of the $Zr^{4+}$ and/or $Y^{3+}$ cations) mechanisms controlled by interface-reaction step for high and low effective compaction stresses respectively. For SPS, at low temperatures or low effective compaction stresses when the temperature is higher, sintering seems to proceeds by grain boundary sliding accommodated by an in-series (interface-reaction/lattice diffusion of the $Zr^{4+}$ and/or $Y^{3+}$

cations) mechanism controlled by the interface-reaction step while at the high temperatures, or at high effective compaction stresses for lower temperatures, a dislocation-climb-controlled mechanism assisted by grain boundary sliding was active.
Bernard-Granger *et al.* further indicate that these differences in sintering mechanisms lead to different microstructures for the samples sintered by SPS compared to those sintered by HP, which can explain why even if the relative densities and grain sizes are similar, the ionic conductivity of the SPS samples is greater than those sintered by HP

Some of us have also investigated the SPS densification mechanisms of an undoped commercial $\alpha$-$Al_2O_3$ powder (0.14 μm) [17]. A sintering path showing two separate regimes was brought to light: densification without grain growth occurring at the lower temperatures and grain growth without much further densification taking place at the higher temperatures, the threshold being between 1100 and 1200°C (fig. 1a.). In the grain growth regime, increasing the applied pressure tends to favour grain growth, possibly through grain-boundary diffusion. Delaying the moment during the thermal cycle at which pressure was applied produced a small increase in relative density, without any adverse effects on grain size, which could indicate better powder packing because of easier particle sliding or rotation at higher temperatures. Increasing the dwell time at 1000°C (densification regime) produces a regular increase in relative density, reaching 86.1% for 60 min with a grain size of 0.2 μm. The dwell time could thus be used to control the proportion of porosity in the specimen precisely. At 1100°C (grain-growth regime), the relative density also regularly increases upon the increase in dwell time, reaching 99.8% for 60 min with a grain size of 0.5 μm. Changing the pulse pattern while maintaining the other experimental conditions constant did not influence the relative density or the grain size. In the second part of the present study, formal sintering analysis was performed in both the densification and grain-growth regimes. In the densification regime, determination of the stress exponent using the model developed for HP suggests a densification mechanism by grain-boundary sliding or by interface reactions for a low applied pressure (25 MPa). In contrast, for a higher pressure (100 MPa), this analysis points towards dislocation climb or plastic deformation, both of which are unlikely mechanisms for $\alpha$-$Al_2O_3$ in this temperature range, whereas the activation energy of densification (evaluated at 644 kJ $mol^{-1}$) points towards grain-boundary diffusion of the $Al^{3+}$ ions. TEM observation of a selected specimen did not reveal the presence of dislocations, and therefore it is proposed that the HP model is not suitable for SPS, at least for high applied pressures. Particular electrical effects during SPS should probably be considered, involving mechanisms including thermal-diffusion and local softening/melting of the grain surfaces owing to very high local temperatures caused by discharges or by plasma, to account for the fast densification. In the grain-growth regime, the analysis points towards volume diffusion or diffusion through a local liquid phase. The presence of such a liquid phase, or at least softened grain surfaces remains speculative and warrants further study.

More recently, Aman et al. also studied the FAST kinetics of another pure commercial $\alpha$-alumina powder (0.17 μm) [18]. Here again, they were able to obtain highly dense and fine pure polycrystalline $\alpha$-alumina with very short sintering times. They showed that heating rates strongly influenced the sintering mechanisms and kinetics. At low sintering temperatures, densification is strongly favoured by a low heating rate, probably due to grain-boundary diffusion. Instead, a required condition of thermal equilibrium, due to the large thermal gradient at interparticle contacts, could enhance the surface diffusion coefficient and thus grain growth during the initial-stage sintering of fine alumina powder sintered at high heating rates. Regardless of the heating rates, plastic yield might lead to instantaneous densification at an early stage of sintering. At high sintering temperatures ($T1 \geq 1150$°C), grain coarsening is unavoidable because of surface diffusion and pore-controlled boundary migration during the dwell. At high sintering temperatures, the densification rate is much lower for samples heated slowly, probably due to grain-boundary sliding and power-law creep, in contrast to lattice diffusion and grain-boundary sliding for high heating rate samples.

In view of the results presented in these two parallel studies and those published by J. Langer et al. comparing the two techniques (SPS and FAST on different type of ceramics), more investigations should be performed in order to elucidate the real mechanisms involved in the SPS or FAST densification of alumina.

Some of us have also studied the sintering mechanisms of nanocrystalline pure $Y_2O_3$ powders [19,20]. Fully dense specimens were obtained by SPS for 5 min at 100MPa in the temperature range 1100–1600°C (fig. 1b.). Increase in the heating rate up to 180°C.min$^{-1}$ led to increases in both density and grain size. While continuous grain growth was observed with the increase in the SPS temperature, a maximum in density was observed at 1400°C. Based on microstructure observations this maximum is due to competition between densification and enhanced grain growth; the latter dominating above 1400°C. Analysis of the grain growth kinetics and its associated diffusion coefficients and activation energy was in agreement with particle coarsening during the heating up stage, followed by grain boundary diffusion at the SPS temperature. The $Y^{3+}$ grain boundary diffusion coefficients were enhanced by three orders of magnitude compared to the literature data. Nanocrystalline (18nm) $Y_2O_3$ powders were sintered using SPS at 1100°C and 100MPa for different durations. Specimens with 98% density and 106±33nm mean grain size were formed after 20 min. The grain size at the final stage of sintering first increased and then tended towards stagnation with the duration of SPS. The phenomenon was investigated with respect to two possible drag mechanisms: triple junction drag and nano-pore drag. The theoretical approach for triple junction drag developed by Raj and Lange and later extended by Chokshi, based on a non-equilibrium dihedral angle at the triple junction was refined. The present calculations showed that triple junction drag in nanocrystalline $Y_2O_3$ is not significant at relatively low sintering temperatures and unrealistic at high temperatures. Grain growth stagnation was attributed to the presence of nano-pores at grain junctions. The SPS process resulted in almost fully dense specimens but the nano-pores at the grain junctions persisted. A refined model for pore densification and coalescence based on grain boundary diffusion for pore shrinkage and surface diffusion for grain growth was used to determine the critical pore size necessary for grain growth stagnation. The theoretical expectations were in good agreement with the experimental results. Nano-pores were beneficial for stabilizing the ceramic nanostructure, but may be undesirable when manufacturing theoretically dense ceramics. Grain growth stagnation ceased at long SPS durations resulting in rapid grain growth and loss of the nanocrystalline character.

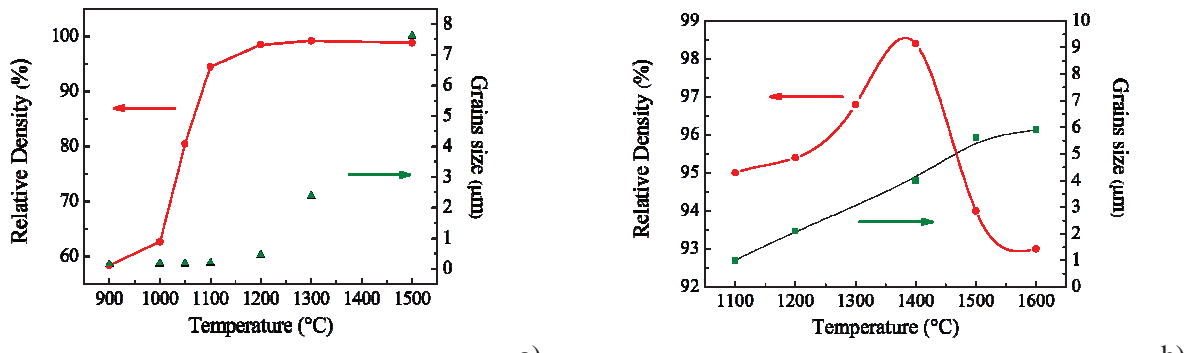


Figure 1: Relative density and average grain size versus the SPS temperature for a) of an undoped commercial α-$Al_2O_3$ powder (140 nm) and b) of a nanocrystalline $Y_2O_3$ powder (18 nm).

It is thus seen that the SPS mechanisms have not yet been perfectly elucidated. Complementary studies will have to be undertaken to determine whether the time saved using this technique allows (over 8 times faster than HP) can be explained solely by the weak inertia of the heating system or whether specific effects must be taken into account.

Below, we briefly illustrate the potential applications of these materials by presenting examples mainly from the literature.

**New transparent materials**

It is well-known that the light intensity transmitted by materials can be attenuated by three mechanisms: absorption, reflexion and diffusion. Thus, optimal density is required to have transparent materials because porosity is one of the main sources of light diffusion. Numerous articles can be found which highlight the ability of SPS to obtain fully dense and transparent materials without any additives. As an example, Chaim *et al.* were able to fully densify (850°C under 150 MPa during 5 min) MgO nanopowders [21]. They obtained discs (12 mms diameter for 1.5 mm thickness) having a transparency from 40% at 550 nm up to 60% at 700 nm compared to that of a monocrystalline MgO. They explain their results by the fact that using SPS the grain size and the porosity present in the densified samples remain at the nanometric scales and do not exceed the wavelength.

**Control of porosity**

SPS is a useful technique to obtain completely densified pieces in relatively short cycle times compared to conventional techniques. The principal parts of the SPS devices are equipped with internal dilatometers to follow the shrinkage of the material and to stop it at any time. It is thus possible to control the sintering of materials (metals or ceramics) and thus to control their level of porosity with or without additives during sintering [22]. Furthermore, Dibandjo *et al.* also showed that SPS can be used to consolidate materials (silica, carbon and boron nitride) to obtain monoliths while preserving the initial mesoporosity of the grains [23].

**Stabilization of metastable elements**

The complete densification of materials by SPS under controlled atmosphere stabilizes metastable elements or phases. Chung et al. and Guillemet-Fritsch et al. thus stabilized $Ti^{3+}$ in barium titanates conferring colossal permittivity to the materials [24,25]. The hydroxyapatites, essential biomaterials because of their good bone adherence, are under employed because of their brittleness. Drouet et al. have consolidated nanocrystalline hydroxyapatites by SPS, yielding materials rather close to bone mineral [26]. The great surface reactivity of this material is related to a metastable hydrated layer present at the surface of the grains. It cannot be sintered by conventional techniques without damaging this layer. Sintering this material by SPS at low temperatures (100-250°C) and under argon allowed the consolidation of this material while preserving the hydrated layer. Gurt et al. also showed that SPS densification of partially reduced metal-oxide nanocomposite powders from solid solution $\alpha$-$Al_{1.86}Fe_{0.14}O_3$ produces nanocomposite materials with a surface layer composition and microstructure different to those of the core of the material. All materials were densified up to 98–100% and the *in situ* composite surface layer formed leads to greater hardness and fracture strength [27].

**Nanomaterial structuration**

As previously mentioned, SPS reduces the temperature and duration of sintering thus allowing grain growth to be controlled. Therefore, many nanomaterials have been successfully sintered by SPS [28,29]. For instance, dense $BaTiO_3$ monoliths were obtained from nanopowders in which the influence of the grain boundaries was minimized leading to remarkable dielectric properties (permittivity at ambient temperatures of 3500 and permittivity with $T_C$ $\varepsilon' > 6000$) [30]. Chesnaud *et al.* used SPS to fully densify refractory nanomaterials of the lanthanum silicate family ($La_{9.33+x}Si_6O_{26+3/2x}$) with grain sizes ranging between 100 and 500nm. However, from the point of view of the conduction properties, the contribution of SPS is not necessarily positive as the values of conductivity are lower than in samples with bigger grain sizes due to the blocking effect of the more numerous grain boundaries in low temperature SPS sintered materials [31].

Single-wall (SWCNT) or multi-wall (MWCNT) carbon nanotubes have extremely interesting mechanical properties (e.g. low density, – Young's modulus higher than $1.10^{12}$Pa). Studies were undertaken to obtain monoliths [32] but they were also considered for use as reinforcement element for ceramics or metals[33]. As an example, dense double-walled carbon nanotubes

(DWCNT)/nanostructured MgO composites (fig. 2) were prepared by spark-plasma-sintering exhibiting an unambiguous increase in both toughness and microhardness [34]. Crack-bridging on an unprecedented scale, crack-deflection and DWCNT pullout were seen to occur. The very long DWCNTs, which appear to be mostly undamaged, were very homogeneously dispersed at the grain boundaries of the matrix, greatly inhibiting grain growth during sintering. These results are due to the unique microstructure (low content of long DWCNTs, nanometric matrix grains and grain boundary cohesion) at the appropriate scale of reinforcement to make the material tough.

**Material assembly through SPS**

Many papers report the ability of SPS to weld parts of materials to obtain momoliths. Due to the lower temperature and the shorter durations achieved during SPS sintering, this technique is also suitable for the preparation of multi- or fully-graded materials owing to the fact that interdiffusion or reaction between two adjacent materials can be limited, favoured or controlled. Therefore properties of parts can be modulated, for instance 2D ($BaTiO_3$/MgO/$BaTiO_3$ sandwich, see fig.3), 3D (MgO+$BaTiO_3$ mixture) and core/shell ($BaTiO_3$@$SiO_2$) architectures have also been prepared by SPS to obtain ferroelectric composite materials presenting low dielectric losses ( < 1%) or high permittivity [35,36]. SPS also allows powders and metallic foils to be combined on substrate to obtain multilayered coatings in a single short production step. Therefore, MCrAlY overlays with local Pt and/or Al enrichments, as well as fabrication of coatings made of ζ-$PtAl_2$, ε-PtAl, α-$AlNiPt_2$, martensitic and β−(Ni,Pt)Al or Pt-rich γ/γ' phases, including their doping with reactive elements have been prepared by SPS on nickel based superalloy subtrates. The fabrication of a complete TBC system (fig. 4.) with a porous and adherent yttria-stabilized zirconia layer on a bond-coating has also been demonstrated [37-39],

**Conclusion**

The use of FAST and SPS techniques has grown significantly over the last decades. They are extremely powerful techniques to sinter all classes of already existing materials (metals, ceramics, polymers) as well as their composites. However, their field of activity also extends to the synthesis, to the assembly, and to the preparation of new materials (nanocomposites, multimaterials, nanoceramics) or graded materials (in composition, microstructure, porosity). These techniques, already practiced in industry, allow technological projections in varied fields notably including power electronics, structural materials, energy storage, biomaterials or aeronautics and space.

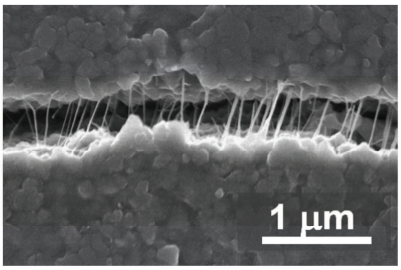


Figure 2: FESEM Image showing a crack bridged by DWCNT in a composite NTC-MgO densified by SPS.

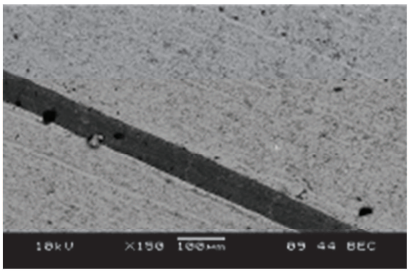

Figure 3: Scanning Electron Microscope Micrograph of a BST64/MgO/BST64 sandwich densified by SPS.

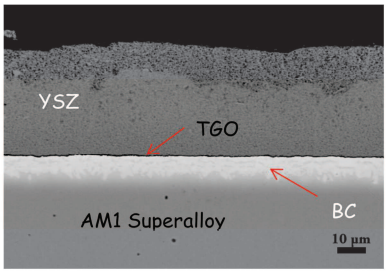


Figure 4: Thermal Barrier Coating system fabricated in one step by SPS from the stacking: AM1, Pt & Al foils and Tosoh TZ8Y powder.

[1] S.H. Risbud, S.-H.Shan, A.K. Mukherjee, M.J. Kim, J.S. Bow, R.A. Holl, J. Mater. Res., 10, 1995, 237.
[2] S.-C. Liao, Y.-J. Chen, B.H. Kear, W.E. Mayo, Nanostruct. Mater., 10, 1998, 1063.
[3] C. Kleinlogel, L.J. Gauckler, Adv. Mater. 13, 2001, 1081.
[4] I.-W. Chen, X.-H.Wang, Nature 404, 2000, 168.
[5] A.G. Bloxam, GB patent 27002, 1906.

[6] A.G. Bloxam, GB Patent 9020, 1906.
[7] R. Orru, R. Licheri, A.M. Locci, A. Cincotti, G. Cao, Mater. Sci. and Eng. R, 63(4-6), 2009, 127.
[8] K. Inoue, US Patent, N° 3 241 956 ,1966.
[9] K. Inoue, US Patent, N° 3 250 892, 1966.
[10] I.J. Shon, A.Z. Munir, Mater. Sci. Engin. **A202,** 1995, 256.
[11] G. Xie, O. Ohashi, M. Song, K. Mitsuishi, K. Furuya, Appl. Surf. Sci. **241,** 2005, 102.
[12] W.M. Goldberger, B. Merkle, D. Boss, Adv. Powder Metall. Particulate Mater **6,** 1994, 91.
[13] M. Tokita, Mater. Sci. Forum **308–311,** 1999, 83.
[14] E.A. Olevsky, S. Kandukuri, L. Froyen, J. of Appl. Phys. 102, 2007, 114913-1-12.
[15] E.A. Olevsky, L. Froyen, Scripta Materialia 55,2006, 1175.
[16] G. Bernard-Granger, A. Addad, G. Fantozzi, G. Bonnefont, C. Guizard, D. Vernat, Acta Materialia, 58(9), 2010, 3390.
[17] J. Gurt-Santanach, A. Weibel, C. Estournès, Q. Yang, Ch. Laurent, A. Peigney, Acta Materialia, 59 (4), 2011, 1400.
[18] Y. Aman, V. Garnier, E. Djurado, J. of the Amer. Ceram. Soc., online: 14 MAR 2011.
[19] R. Chaim, A. Shlayer, C. Estournes, J. of the Europ. Ceram. Soc., 29(1), 2009, 91.
[20] R. Marder, R. Chaim, C. Estournès, Materials Science and Engineering: A, 527(6), 2010, 1577.
[21] R. Chaim, Z. Shen, M. Nygren, J. Mater. Res. 19 (2004) 2527.
[22] P.O. Vasiliev, Z. Shen, R.P. Hodgkins, L. Bergström, Chem. Mater., **18** (20), 2006, 4933.
[23] P. Dibandjo, L. Bois, C. Estournes, B. Durand, Ph. Miele, Microporous and Mesoporous Materials 111, 2008, 643.
[24] U.-C. Chung, C. Elissalde, S. Mornet, M. Maglione, C. Estournès, Applied Physics Letters, 94(7), (2009), 072903.
[25] S. Guillemet-Fritsch, Z. Valdez-Nava ,C. Tenailleau , T. Lebey , B. Durand , J.-Y. Chane-Ching, Adv. Mater. 20, 2008, 551.
[26] D. Grossin, S. Rollin-Martinet, C. Estournès, F. Rossignol, E. Champion, C. Combes, C. Rey, G. Geoffroy, C. Drouet, Acta Biomaterialia, 6(2), 2010, 577.
[27] J. Gurt-Santanach, C. Estournès, A. Weibel, A. Peigney, G. Chevallier, Ch. Laurent, Scripta Materialia, 60(4), 2009, 195.
[28] A.V. Ragulya, Adv. in Appl. Ceram., 107(3) 2008, 118.
[29] R. Chaim, M. Levin, A. Shlayer, C. Estournes, Adv. in Appl. Ceram. 107(3) 2008, 159.
[30] T. Takeuchi, Y. Suyama, D. C. Sinclair, H. Kageyama, J. Mater. Science 36 (2001) 2329
[31] A. Chesnaud , G. Dezanneau, C. Estournès, C. Bogicevic, F. Karolak, S. Geiger , G. Geneste, Solid State Ionics, 179 [33-34], 2008, 1929.
[32] Ch. Laurent, G. Chevallier, A. Weibel, A. Peigney, C. Estournès, Carbon, 46(13),2008, 1812.
[33] A. Peigney, Nature Materials 2 (2003) 15.
[34] A. Peigney, F. Legorreta Garcia, C. Estournès, A.Weibel, Ch. Laurent, Carbon, 48 (7), 2010, 1952.
[35] C. Elissalde, C. Estournès, M. Maglione, J. Amer. Ceram. Soc., 90 (3), 2007, 973.
[36] U.-C. Chung, C. Estournès, C. Elissalde, M. Paste, J.P. Ganne, M. Maglione, Applied Physics Letters, 92 (4), 2008, 042902/1.
[37] D. Oquab, C. Estournes, D. Monceau, Advanced Engineering Materials 9(5), 2007, 413.
[38] D. Oquab, D. Monceau, Y. Thebault, C. Estournès, Materials Science Forum Vols 595-598 2008, 143.
[39] D. Monceau, D. Oquab, C. Estournes , M. Boidot, S. Selezneff, Ratel-Ramond, Materials Science Forum Vols. 654-656, 2010, 1826.